Journal of Ultrafine Grained and Nanostructured Materials
https://jufgnsm.ut.ac.ir
Vol. 56, No.2, December 2023, pp. 147-156
Print ISSN: 2423-6845 Online ISSN: 2423-6837
DOI: 10.22059/jufgnsm.2023.02.03

Microstructure and mechanical properties in dissimilar friction stir welding of 316 stainless steel to 4140 steel

Ali Malekan[1], Mehdi Malekan[*,2], N. Banimostafa Arab[1], Hossein Bayat Tork[1]

[1]Department of Mechanical Engineering, Shahid Rajaee Teacher Training University (SRTTU), Lavizan, Tehran, Iran;
[2]School of Metallurgy and Materials Engineering, College of Engineering, University of Tehran, P.O. Box 11155-4563, Tehran, Iran.

Recieved: 30 July 2023; Accepted: 4 December 2023

**Corresponding author email: mmalekan@ut.ac.ir*

ABSTRACT

In the current study, 316 stainless steel and 4140 steel sheets were successfully joined using friction stir butt welding (FSBW). The tool's rotational speed and the linear welding speed were assumed to be 1400-1700 rpm and 30-50 mm/min, respectively. The weld microstructures were examined by X-ray diffraction (XRD), optical microscopy, and scanning electron microscopy (SEM). In this welding, three zones with different structures relative to the base metals, including thermomechanical zones for each base metal and stir zone, were formed. Observations indicated that in the microstructure of 4140 steel containing martensite, the martensite blades vanished, and the grains extended in the thermomechanical zone. Furthermore, in the 316 stainless steel containing austenite, the austenite grain size was shrunk due to the dynamic recrystallization in the thermomechanical zone. Also, the microhardness test results showed that the stir zones have higher hardness than base metals in all specimens because of the dynamic recrystallization and fine-grained structure. Moreover, the 1550 rpm - 40 mm/min welded specimen in the stir zone has the highest yield strength of 350 MPa in the tensile test, which was higher than the yield strength of 316 stainless steel.

Keywords: *Friction stir welding; mechanical properties; microstructure; 316 stainless steel; 4140 steel.*

1. Introduction

Dissimilar welding of metals has turned into a critical technology in numerous areas where both strength and corrosion resistance are required [1, 2]. The Joining of dissimilar metal combinations are utilized in various applications requiring specific combinations of weldment properties and saving cost [3,4]. The dissimilar metal welding gives possibilities to the item's versatile plan by using each material effectively and efficiently, i.e., benefitting from each material's specific properties [5].

Dissimilar welds of stainless steel and low alloy steel are required when changes in mechanical properties and service performance are required [6]. For welds of carbon and austenitic steel, it is feasible to notice harm in the austenitic steel, which is basically the material with better corrosion resistance. This self-contradictory peculiarity is attempted to be brought about by the segregation of impurities i.e. S, P, and C from carbon steel on austenitic grain boundaries. Unfortunately, it might

likewise be a source of functional issues because of joining at least two metals with various corrosion resistance [7]. Power generation equipment such as fossil fuel boilers and steam generators, water walls surrounding furnaces, economizer assemblies, and superheater and reheater front and rear sections are equipment where dissimilar welds of stainless steel to low alloy steel are an example of widely applications. [8].

The process of welding different steel alloys is very complicated since the alloy gradient. Hence, the migration of carbon from the low-alloy side can result in variation of microstructure, residual stress and brittle intermetallic compounds (IMCs) in various districts of the weld metal [1, 2]. When welding stainless steel to low-alloy steel, there is a risk of cold cracking due to the formation of martensite in the weld zone after dilution with the base metal and residual ferrite. Also, hot cracking may happen by the low melting point impurities, e.g., phosphor and sulfur [1, 6, 9, 10]. In addition, due to the significant difference in chemical compositions, there is a high risk of affecting the mechanical properties when melting both stainless and low alloy steels using fusion welding processes, e.g., gas metal arc welding and gas tungsten arc welding [11]. Unfortunately, welding these metals together by other methods is very complicated and difficult.

Dissimilar metals are typically less weldable than similar metals due to poor joint design, formation of other intermetallic compounds, differences in metal composition, and differences in mechanical and thermal properties [12]. Low alloy filler metals in austenitic stainless steels can lead to brittle and hard weld deposits. Carbon diffusion and subsequent formation of detrimental carbides in the weld metal is important when joining low-alloy and carbon steels to stainless steel. Therefore, decarburization and grain growth occur in the heat-affected zone (HAZ) of carbon steel, affecting mechanical properties [7].

Consequently, many researches are conducted on the possibility of joining dissimilar materials utilizing friction stir welding (FSW) [13,24]. Friction stir welding is a generally new method that utilizes non-consumable tools to generate frictional heat and plastic deformation so that the formation of the joint in its solid state is affected and joins two metals in the solid-state [25,28] and as a result of actively controlling the welding temperature and/or cooling rate, FSW can produce steel joints with great toughness and strength [29]. This method is a solid state hot shear joining method using rotating tools [30-31], and was first used by TWI (The Welding Institute) in Cambridge, England (1991) and used for welding the aluminum alloys [25-27, 32].

The invention of friction stir welding (FSW) is an innovative and newly defined solid material joining process for lightweight structures [33]. The study of welding dissimilar materials is of great interest to scientists and engineers. The demand to develop lightweight, strong, improved electrical properties and cost-effective mechanical parts or structures is continuously increasing in various industries [34]. The advantages of FSW for dissimilar joining of various alloys are demonstrated in several publications [35,40].

FSW of stainless steels [36, 41,43] and carbon steels [44,46] has yielded very encouraging outcomes and has shown that this welding technique has several advantages. However, dissimilar FSW of stainless steels to carbon or alloy steels is not investigated adequately. An instance of stainless steel-carbon steel FSW illustrated the presence of four various microstructures within the weld area, i.e., heat-affected zone (HAZ) of St37, thermomechanically affected zone (TMAZ) of AISI 304 SS, and stir zones (SZ) of both materials. In contrast, the weld center contained alternating bands of the microstructures of both steels. It is also reported that due to hot deformation associated with the FSW process, hence, recrystallization of austenite in the SZ region, the austenite was transformed to ferrite-pearlite and Widmanstatten ferrite. In addition, the increase of hardness in the weld SZ is attributed to the dynamic recrystallization of austenite in these regions [13].

It is well known that the weld microstructure is firmly impacted by the welding variables. However, the effects of FSW parameters on the microstructure and properties of various welds of stainless steels and carbon and low-alloy steels are not well understood.

The purpose of this study was to investigate the effects of welding parameters on the microstructure and mechanical properties of FSW from 316 stainless steel to 4140 steel. Using microscopy and analytical techniques, it has investigated the microstructure of different zones of the weld. Mechanical properties were also investigated by tensile and hardness tests.

2. Experimental procedure

In the current study, 316 austenitic stainless steel and 4140 quench-tempered steel with the chemical composition obtained by emission spectroscopy in Table 1 were used as base metals.

A sheet of 100 mm x 100 mm with a 2 mm thickness was prepared for friction stir butt welding. A cylindrical tungsten carbide pin was used as the welding tool. The shoulder diameter, pin length, and pin diameter were considered 20 mm, 1.8 mm, and 3 mm, respectively. In addition, FSW was performed at rotational speeds of 1400, 1550, and 1700 rpm and linear speeds of 30, 40, and 50 mm/min. A schematic of the FSW technique is shown in Figure 1.

Research studies on FSW have demonstrated that the advancing side sheet experiences higher temperatures [47,49]; therefore, stronger metal is placed in the advancing side to achieve the desired flow at the joint. Hence, 4140 steel is stronger than 316 stainless steel, so it was put 4140 steel in the advancing side and 316 stainless steel in the retreating side.

The metallographic specimens were prepared from the horizontal top surface of the weld, which included the two base metals and their joints. After polishing the specimens, according to the ASTM E3 standard [50], nital 2 % solution was first used for etching the 4140 steel; then, the 316 stainless steel was etched with the nitric acid 60 % solution via electrolytic etching. This method is characterized by the feature that the electrolytic etching of 316 stainless steel does not affect 4140 steel. Microstructures were observed and analyzed by optical microscope (OM) and Vega Tescan scanning electron microscope (SEM) outfitted with energy-dispersive spectroscopy (EDS). Moreover, the grain size was calculated using the MLI (Mean Linear Intercept) method. Also, Phase identification was performed by the X-ray diffraction (XRD) technique using a PHILIPS diffractometer with the Cu-kα radiation.

The tensile specimens were prepared perpendicular to the welding direction (transverse tensile test) based on the ASTM E8 standard [51]. Tensile tests were performed on an Instron 5500R

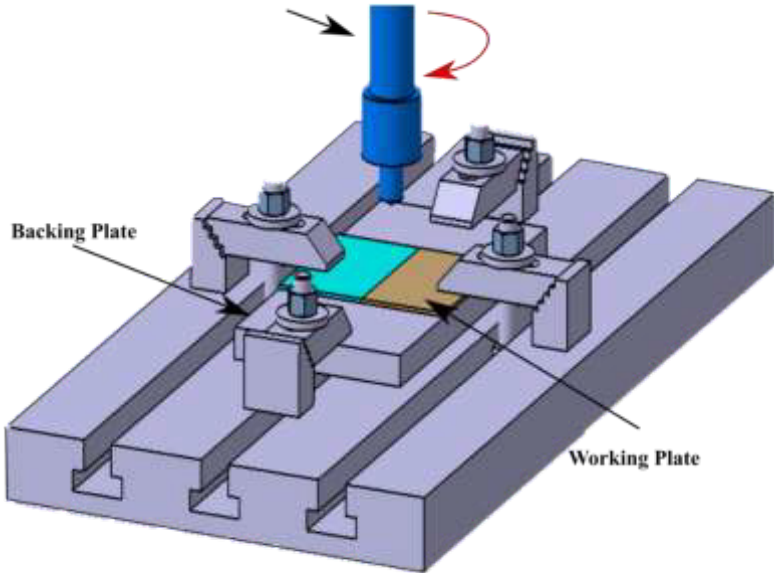

Fig. 1- Schematic drawing of FSW technique for welding 316 stainless steel to 4140 steel.

Table 1- The chemical composition of 316 stainless steel and 4140 steel

Alloy	Wt.%									
	Nb	S	P	Mo	Ni	Cr	Mn	Si	C	Fe
316 stainless steel	0.02	0.01	0.04	1.64	10.42	17.22	1.37	0.43	0.04	Bal.
4140 steel	-	0.01	0.01	0.19	0.03	0.90	0.78	0.28	0.39	Bal.

machine at ambient temperature with a strain rate of 5 x 10-4 s-1. Three tensile specimens were tested at each condition to achieve reasonable reliability. In addition, the fracture surface of the tensile specimen was observed with SEM to investigate the fracture mode. The hardness of the samples was measured along the middle line of the cross section perpendicular to the weld path with a load of 100 g for 15 seconds and a point spacing of 2 mm.

3. Results and discussion

3.1. Microstructural characterization

Fig. 2 shows the microstructures of different zones of 316 stainless steel-4140 steel FSW at 1400 rpm and 40 mm/min. As should be visible, the 316 stainless steel as one of the base metals has an austenitic structure, in which the flow lines resulting from cold rolling operation during the production process can be observed. Coaxial grains containing ferrite residues can also be observed in the 316 SS base metal [52]. The grain size on this side decreases from 13 µm in the substrate to 8 µm in the thermomechanically affected zone (TMAZ) and 3 µm in the stir zone (SZ) (Table 2). Such grain size reduction is caused by dynamic recrystallization due to heat input and force and is different for each specimen under different conditions.

The other side is 4140 steel, which has a martensitic microstructure in the base metal zone (Fig. 2) so that the martensitic blades are visible. Still, in the zones close to the line joining the two metals (SZ and TMAZ), this structure is converted into a tempered martensitic structure. When the martensitic structure is affected by the pin's stirring, the development of martensitic occurs along with the growth and arrangement of the grains as a result of suitable thermal distribution [53].

As can be observed, increasing the rotational

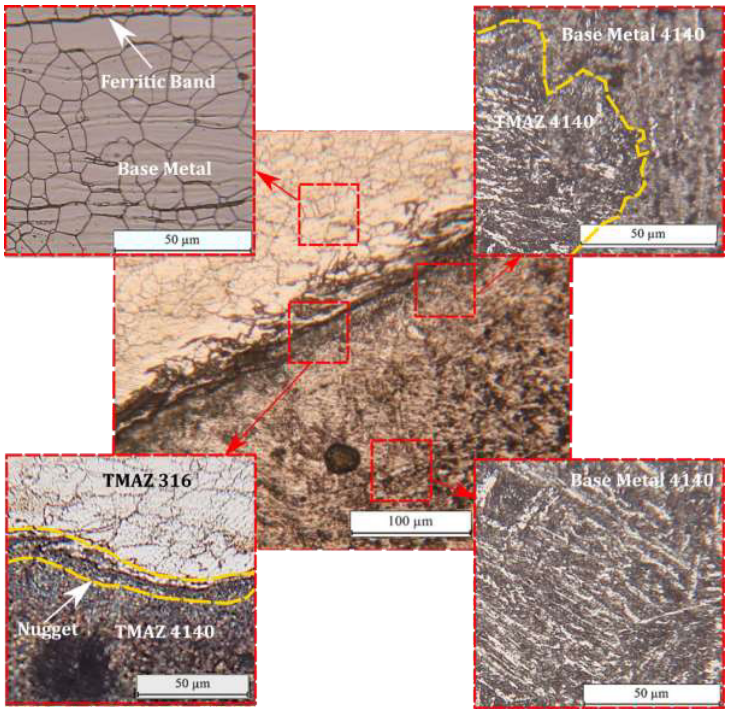

Fig. 2- Optical microstructures of the different zones of 316 stainless steel-4140 steel FSW at a speed of 1400 rpm and 40 mm/min.

Table 2- Average grain size (µm) in SZ and TMAZ

	1400 rpm 40 mm/min	1550 rpm 40 mm/min	1700 rpm 40 mm/min	1550 rpm 30 mm/min	1550 rpm 50 mm/min
SZ	3	6	7	5	6
TMAZ	8	9	10	8	8

speed of the tool from 1400 to 1700 rpm at a constant linear speed of 40 mm/min increases the particle size from 3 μm to 7 μm due to the temperature increase during stirring. This increase in the grain size exhibits lower variations in the TMAZ. Grain size reduction in the stirred zone is the consequence of the dynamic recrystallization phenomenon. Moreover, at a constant rotational speed of 1550 rpm, the grain size does not show much change with changing the linear velocity of the FSW.

Fig. 3 shows the SEM micrograph of an FS-welded specimen in the stirred zone along with EDS linear analysis. As can be seen, 316 stainless steel is observed on the light side and 4140 steel is observed on the dark side.

Besides, the red line specifies the EDS analysis path. The EDS linear analysis shows the penetration path of nickel and chromium from 316 stainless steel toward 4140 steel and the penetration path of iron and carbon from 4140 steel toward 316 stainless steel, which is indicative of a proper joint.

Fig. 4 shows the XRD analysis in the stirred zone of the FS-welded specimens. The peaks shown in the patterns are related to the austenite phase. In this study, no new phases formed in the stir zone and the phases present are related to 316 stainless steel.

3.2. Mechanical properties

Fig. 5 shows the micro-hardness profile of the FS-welded specimens. The results in Fig. 5a indicate that microhardness values in the SZ and TMAZ zones increase rather than base metals due to the reduced grain size resulting from fragmentation of grains and dynamic recrystallization. Besides, Vickers microhardness values in the base metals are about 222 for the 4140 steel and 210 for the 316 stainless steel. The Vickers microhardness values in the SZ and TMAZ zones are in the range of 250-350. As the tool speed increases, the heat input to the workpiece increases, so the hardness values in the SZ and TMAZ zones decrease and the grains grow. The microhardness values at a constant tool rotational speed of 1550 rpm in Fig. 5b indicate the maximum hardness for the 1550rpm-30mm/min, 1550rpm-40mm/min, and 1550rpm-50mm/min specimens are 332, 320, and 304 Vickers, respectively. Moreover, increasing the linear speed at the constant tool rotational speed indeed decreases the heat input, which would lead to reduced hardness in the SZ zone.

FSW causes considerable changes in the strength of welding specimens. These changes can

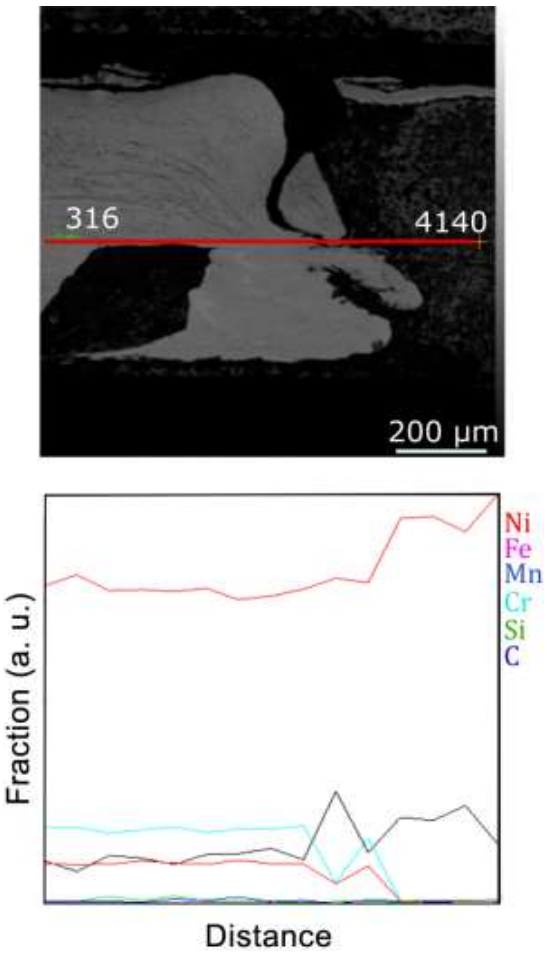

Fig. 3- SEM micrograph and linear EDS analysis of FS welded sample at 1550 rpm - 40 mm/min.

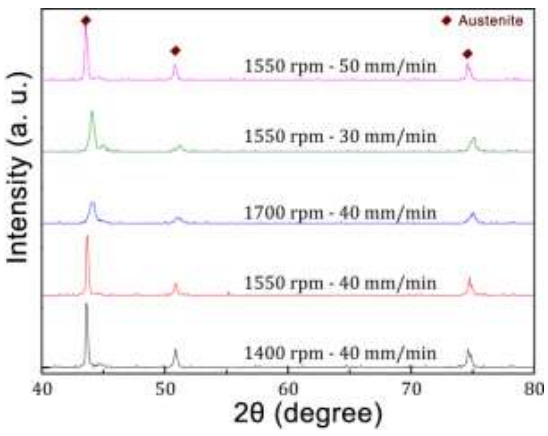

Fig. 4- XRD analysis of stirred zone of FS-welded specimens.

be seen in the tensile test results. Fig. 6 shows the stress-strain curves derived from the tensile test of the FS-welded specimens. As can be seen, the 1550rpm-40mm/min specimen has the best tensile properties with the yield strength (YS) and ultimate tensile strength (UTS) of 350 MPa and 440 MPa, respectively. The yield strength of the 1550rpm-40mm/min specimen is higher than that of 316 stainless steel base metals and lower than that of the 4140 steel, but the UTS is less than both base metals. Figure 7 shows the tensile test results of the FS welded samples.

As shown in Fig. 7, Elongation (El) is directly proportionate to the heat input; in fact, the elongation of the tensile specimens reduces by decreasing the grain size. The highest El of 25% is related to the 1700 rpm - 40 mm/min specimen, while the 1400rpm-40mm/min specimen has the lowest El of 11%.

Fig. 8 shows the tensile fracture surface of the FS-welded specimens. The transverse tensile specimens are consisted of base metals, HAZ, TMAZ and stir zone, which their fracture occurred from stir zone. Fig. 8a represents that the tensile fracture of the 1400 rpm - 40 mm/min specimen is a brittle type because of some features such as cleavage facets, steps, and microcracks. As shown in Fig. 8d, the reason for the disjoint at the weld site is the presence of tunnel defects. The low heat input compared to other specimens could cause such defects and inappropriate joints.

According to Fig. 8b, the fracture mode with increasing the rotational tool speed to 1550 rpm is almost similar to that of the 1400 rpm – 40 mm/min specimen. Moreover, the surface has fewer superficial defects and microcracks. In Fig. 8c, by increasing the rotational tool speed to 1700 rpm and increasing the heat input, the specimen underwent a ductile fracture. Besides, in this specimen, the El% was the highest among other specimens. Ductile fracture is formed through the connection and conjoining of small dimples that germinated in the strain discontinuous regions such as inclusions, grain boundaries, and accumulation

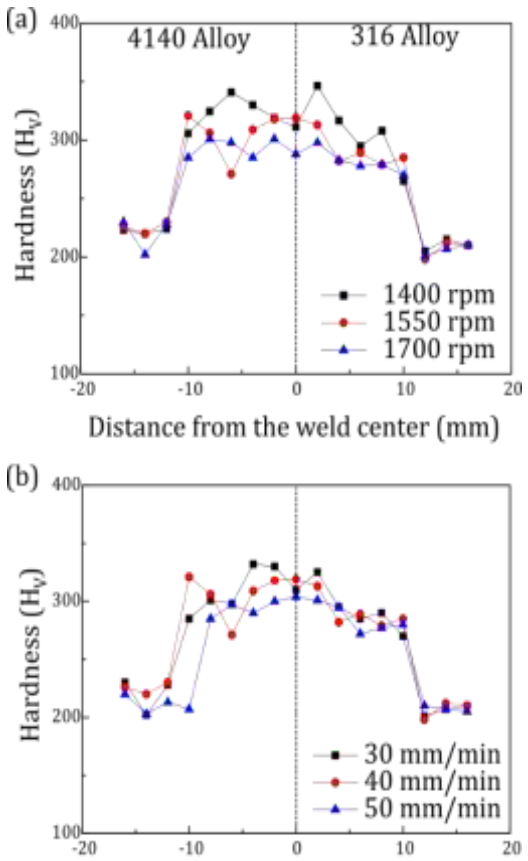

Fig. 5- Microhardness profile of the FS-welded specimens (a) at a constant linear speed of 40 mm/min; (b) at a constant tool rotational speed of 1550 rpm.

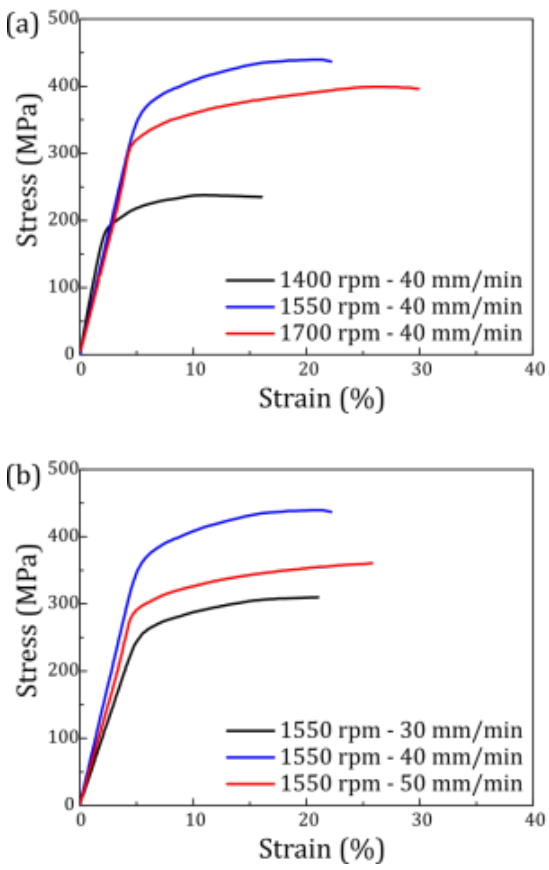

Fig. 6- Microhardness profile of the FS-welded specimens (a) at a constant linear speed of 40 mm/min; (b) at a constant tool rotational speed of 1550 rpm.

of dislocations. The distribution and size of these small dimples affected the fracture's surface [45]. The dimples are of edged conical type.

4. Conclusion

In this study, the effects of welding parameters on the microstructure and mechanical properties

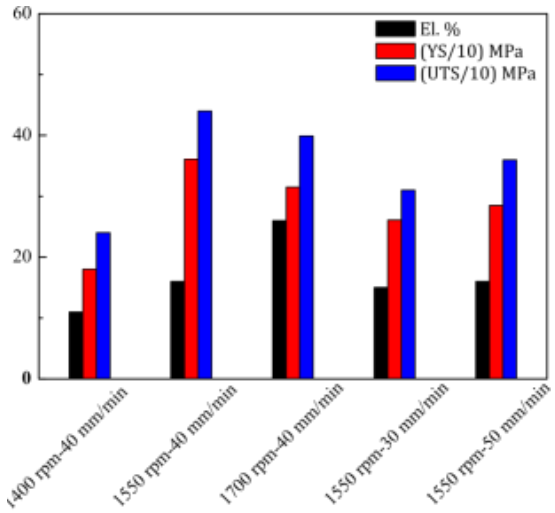

Fig. 7- Comparison of tensile properties of FS-welded specimens.

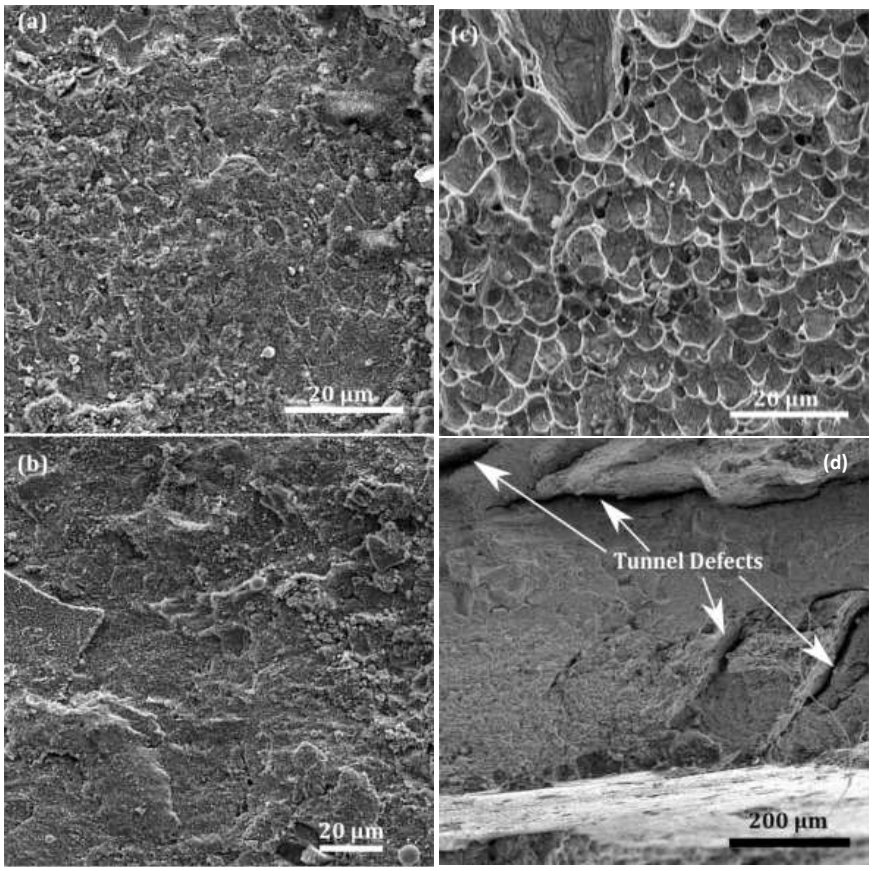

Fig. 8- SEM micrographs of fracture surface of FS-welded specimens in conditions of (a,d) 1400 rpm – 40 mm/min, (b) 1550 rpm – 40 mm/min, (c) 1700 rpm – 40 mm/min.

of FSW of 316 stainless steel to 4140 steel were investigated. The following conclusions were drawn:

-In friction stir welding, the microstructure of 316 stainless steel did not change from the austenitic state in the base metal. Still, in the stir zones, it became finer-grained due to the severe plastic deformation and hence fragmentation of grains. Furthermore, on the 4140 steel side, the structure was changed from the martensitic state in the base metal to a tempered martensitic state in the stir zone.

-Grain size increased with increasing the rotational tool speed from 1700 to 1400 rpm (at a linear welding speed of 40 mm/min) because of more heat input applied to the specimen. However, no significant grain size change was observed with increasing the linear speed from 30 to 50 mm/min (at a constant rotational speed of 1550 rpm).

-The smallest grain size, 3 μm, was obtained in the stirred zone of the FSWed specimen at 1400 rpm - 40 mm/min, while the largest grain size in the stirred zone was 7 μm for 1700 rpm - 40 mm/min specimen.

-XRD analysis of the stirred zone in all specimens indicated the presence of an austenitic phase.

-The hardness of the stirred zone and TMAZ was higher than that of the base metals due to the fine-grained structure. The increased dislocation density, as well as the secondary grains, led to increased hardness. The maximum hardness in the stirred zone was equal to 346 Vickers for the 1440 rpm – 40 mm/min specimen that had the finest-grained specimen in the stir zone.

-With reducing the heat input, the tunnel defects emerged like global pores in the weldment, attributed to the low flow.

-Tunnel defects and fine-grained structure led to the reduced El% compared to the base metal so that the 1400 rpm - 40 mm/min specimen exhibited the lowest elongation (11%) as the result of the tunnel defects.

-The 1550 rpm – 40 mm/min FSWed specimen had the best tensile properties with the yield strength (YS) and ultimate tensile strength (UTS) of 350 MPa and 440 MPa, respectively.

Conflicts of interest:

The authors declare no conflict of interest with regard to the submitted manuscript.

Data Availability:

All data generated or analyzed during this study are included in this published article.

References

1. Mvola B, Kah P, Martikainen J. Dissimilar ferrous-nonferrous metal welding. Advanced Materials and Information Technology Processing; 2014/02/01: WIT Press; 2014.
2. Praveen P, Yarlagadda PKDV. Meeting challenges in welding of aluminum alloys through pulse gas metal arc welding. Journal of Materials Processing Technology. 2005;164-165:1106-12.
3. Pouraliakbar H, Hamedi M, Kokabi AH, Nazari A. Designing of CK45 carbon steel and AISI 304 stainless steel dissimilar welds. Materials Research. 2013;17(1):106-14.
4. Paventhan R, Lakshminarayanan PR, Balasubramanian V. Fatigue behaviour of friction welded medium carbon steel and austenitic stainless steel dissimilar joints. Materials & Design. 2011;32(4):1888-94.
5. Maurya AK, Pandey C, Chhibber R. Dissimilar welding of duplex stainless steel with Ni alloys: A review. International Journal of Pressure Vessels and Piping. 2021;192:104439.
6. Reddy MP, William AAS, Prashanth MM, Kumar SNS, Ramkumar KD, Arivazhagan N, Narayanan S. Assessment of Mechanical Properties of AISI 4140 and AISI 316 Dissimilar Weldments. Procedia Engineering. 2014;75:29-33.
7. Bystrianský V, Bystrianský J, Dumská K, Macák J, Návoj A. Effect of impurities in dissimilar metal welds on their corrosion behavior. Materials and Corrosion. 2021;72(8):1370-6.
8. Soldering and brazing. Welding Processes Handbook: CRC Press; 2003.
9. Abu-Aesh M, Taha M, Salem El–Sabbagh A, Dorn L. A Proposed Mechanism of Hot-Cracking Formation During Welding Fan-Shaped Test Specimen Using Pulsed-Current Gas Tungsten Arc Welding Process. Engineering and Applied Sciences. 2021;6(5):86.
10. Wang Y, Tsutsumi S, Kawakubo T, Fujii H. Microstructure and mechanical properties of weathering mild steel joined by friction stir welding. Materials Science and Engineering: A. 2021;823:141715.
11. Logan BP, Toumpis AI, Galloway AM, McPherson NA, Hambling SJ. Dissimilar friction stir welding of duplex stainless steel to low alloy structural steel. Science and Technology of Welding and Joining. 2016;21(1):11-9.
12. Devaraj J, Ziout A, Abu Qudeiri JE. Dissimilar Non-Ferrous Metal Welding: An Insight on Experimental and Numerical Analysis. Metals. 2021;11(9):1486.
13. Jafarzadegan M, Feng AH, Abdollah-zadeh A, Saeid T, Shen J, Assadi H. Microstructural characterization in dissimilar friction stir welding between 304 stainless steel and st37 steel. Materials Characterization. 2012;74:28-41.
14. Jamshidi Aval H, Serajzadeh S, Kokabi AH, Loureiro A. Effect of tool geometry on mechanical and microstructural behaviours in dissimilar friction stir welding of AA 5086–AA 6061. Science and Technology of Welding and Joining. 2011;16(7):597-604.
15. Kasai H, Morisada Y, Fujii H. Dissimilar FSW of immiscible materials: Steel/magnesium. Materials Science and Engineering: A. 2015;624:250-5.
16. Aghaei A, Dehghani K. Characterizations of friction stir welding of dissimilar Monel400 and stainless steel 316. The

International Journal of Advanced Manufacturing Technology. 2014;77(1-4):573-9.
17. Karlsson L, Berqvist EL, Larsson H. Application of Friction Stir Welding to Dissimilar Welding. Welding in the World. 2002;46(1-2):10-4.
18. Shen C, Zhang J, Ge J. Microstructures and electrochemical behaviors of the friction stir welding dissimilar weld. Journal of Environmental Sciences. 2011;23:S32-S5.
19. Ishida K, Gao Y, Nagatsuka K, Takahashi M, Nakata K. Microstructures and mechanical properties of friction stir welded lap joints of commercially pure titanium and 304 stainless steel. Journal of Alloys and Compounds. 2015;630:172-7.
20. DebRoy T, Bhadeshia HKDH. Friction stir welding of dissimilar alloys – a perspective. Science and Technology of Welding and Joining. 2010;15(4):266-70.
21. Rodriguez J, Ramirez AJ. Friction stir welding of mild steel to alloy 625 – development of welding parameters. Science and Technology of Welding and Joining. 2014;19(4):343-9.
22. Raj S, Biswas P. Mechanical and microstructural characterizations of friction stir welded dissimilar butt joints of Inconel 718 and AISI 204Cu austenitic stainless steel. Materials Characterization. 2022;185:111763.
23. Sarkari Khorrami M, Saito N. On the formation of large grain structure after friction stir processing of ultrafine-grained aluminium alloy. Philosophical Magazine. 2023;103(8):733-48.
24. Heidarzadeh A, Mironov S, Kaibyshev R, Çam G, Simar A, Gerlich A, et al. Friction stir welding/processing of metals and alloys: A comprehensive review on microstructural evolution. Progress in Materials Science. 2021;117:100752.
25. Mirzadeh H. 'Superplasticity of fine-grained austenitic stainless steels: A review'. Journal of Ultrafine Grained and Nanostructured Materials 2023, 56(1), 27-41.
26. Liu X, Lan S, Ni J. Analysis of process parameters effects on friction stir welding of dissimilar aluminum alloy to advanced high strength steel. Materials & Design. 2014;59:50-62.
27. Guo J, Gougeon P, Chen XG. Microstructure evolution and mechanical properties of dissimilar friction stir welded joints between AA1100-B4C MMC and AA6063 alloy. Materials Science and Engineering: A. 2012;553:149-56.
28. Naghizadeh M, Mirzadeh H. Processing of fine grained AISI 304L austenitic stainless steel by cold rolling and high-temperature short-term annealing. Materials Research Express. 2018;5(5):056529.
29. Liu FC, Hovanski Y, Miles MP, Sorensen CD, Nelson TW. A review of friction stir welding of steels: Tool, material flow, microstructure, and properties. Journal of Materials Science & Technology. 2018;34(1):39-57.
30. Kumar J, Majumder S, Mondal AK, Verma RK. Influence of rotation speed, transverse speed, and pin length during underwater friction stir welding (UW-FSW) on aluminum AA6063: A novel criterion for parametric control. International Journal of Lightweight Materials and Manufacture. 2022;5(3):295-305.
31. Meng X, Huang Y, Cao J, Shen J, dos Santos JF. Recent progress on control strategies for inherent issues in friction stir welding. Progress in Materials Science. 2021;115:100706.
32. Yugandha K, Balaji PS, Chandu P, Prasanna RV, Magesh MN, Loganathan TG. A STUDY ON FSW PARAMETERS OF JOINING DISSIMILAR METALS - AL AND FE. International Journal Of Trendy Research In Engineering And Technology. 2022;06(01).
33. Sejani D, Li W, Patel V. Stationary shoulder friction stir welding – low heat input joining technique: a review in comparison with conventional FSW and bobbin tool FSW. Critical Reviews in Solid State and Materials Sciences. 2021;47(6):865-914.
34. Isa MSM, Moghadasi K, Ariffin MA, Raja S, Muhamad MRb, Yusof F, et al. Recent research progress in friction stir welding of aluminium and copper dissimilar joint: a review. Journal of Materials Research and Technology. 2021;15:2735-80.
35. Saeid T, Abdollah-zadeh A, Shibayanagi T, Ikeuchi K, Assadi H. On the formation of grain structure during friction stir welding of duplex stainless steel. Materials Science and Engineering: A. 2010;527(24-25):6484-8.
36. Emami S, Saeid T, Khosroshahi RA. Microstructural evolution of friction stir welded SAF 2205 duplex stainless steel. Journal of Alloys and Compounds. 2018;739:678-89.
37. Nandan R, Debroy T, Bhadeshia H. Recent advances in friction-stir welding – Process, weldment structure and properties. Progress in Materials Science. 2008;53(6):980-1023.
38. Lakshminarayanan AK, Balasubramanian V, Salahuddin M. Microstructure, Tensile and Impact Toughness Properties of Friction Stir Welded Mild Steel. Journal of Iron and Steel Research International. 2010;17(10):68-74.
39. McPherson NA, Galloway AM, Cater SR, Hambling SJ. Friction stir welding of thin DH36 steel plate. Science and Technology of Welding and Joining. 2013;18(5):441-50.
40. Shafiei-Zarghan A., Najafi A., Kashani-Bozorg S.F. and Zarei-Hanzaki A. 'Effect of Zener-Hollomon Parameter on Microstructure of Aluminum Based Nanocomposite Layers Produced by Friction Stir Processing'. Journal of Ultrafine Grained and Nanostructured Materials 2021, 54(1), 29-39.
41. Mondal M, Das H, Ahn EY, Hong ST, Kim M-J, Han HN, Pal TK. Characterization of friction stir welded joint of low nickel austenitic stainless steel and modified ferritic stainless steel. Metals and Materials International. 2017;23(5):948-57.
42. Kumar SS, Murugan N, Ramachandran KK. Microstructure and mechanical properties of friction stir welded AISI 316L austenitic stainless steel joints. Journal of Materials Processing Technology. 2018;254:79-90.
43. ahl sarmadi m, shamanian m, edris h, behjat a, atapoor m, Szpunar J, Mohtadi Bonab MA. Friction stir welding super duplex stainless steels UNS S32750 and evaluation of microstructure, mechanical and corrosion properties. Journal of Advanced Materials In Engineering. 2017;36(1):97-120.
44. Sun Y, Fujii H. Improved resistance to hydrogen embrittlement of friction stir welded high carbon steel plates. International Journal of Hydrogen Energy. 2015;40(25):8219-29.
45. Khodir SA, Morisada Y, Ueji R, Fujii H. Microstructures and mechanical properties evolution during friction stir welding of SK4 high carbon steel alloy. Materials Science and Engineering: A. 2012;558:572-8.
46. Chung YD, Fujii H, Ueji R, Tsuji N. Friction stir welding of high carbon steel with excellent toughness and ductility. Scripta Materialia. 2010;63(2):223-6.
47. Watanabe T, Takayama H, Yanagisawa A. Joining of aluminum alloy to steel by friction stir welding. Journal of Materials Processing Technology. 2006;178(1-3):342-9.
48. Chung YD, Fujii H, Sun Y, Tanigawa H. Interface microstructure evolution of dissimilar friction stir butt welded F82H steel and SUS304. Materials Science and Engineering: A. 2011;528(18):5812-21.
49. Bang H, Bang H, Jeon G, Oh I, Ro C. Gas tungsten arc welding assisted hybrid friction stir welding of dissimilar materials Al6061-T6 aluminum alloy and STS304 stainless steel. Materials & Design. 2012;37:48-55.
50. A. Standard, "E3, Standard guide for preparation of metallographic specimens," West Conshohecken, PA ASTM Int., 2017. ASTM E8 "Standard test method for tension testing of metallic materials" 2016.
51. ASTM E8 "Standard test method for tension testing of metallic materials" 2016.

52. Odnobokova M, Kipelova A, Belyakov A, Kaibyshev R. Microstructure evolution in a 316L stainless steel subjected to multidirectional forging and unidirectional bar rolling. IOP Conference Series: Materials Science and Engineering. 2014;63:012060.

53. Arivazhagan N, Singh S, Prakash S, Reddy GM. An assessment of hardness, impact strength, and hot corrosion behaviour of friction-welded dissimilar weldments between AISI 4140 and AISI 304. The International Journal of Advanced Manufacturing Technology. 2007;39(7-8):679-89.